



## Comparison of the optical depth of total ozone and atmospheric aerosols in Poprad-Gánovce, Slovakia

Peter Hrabčák<sup>1</sup>

<sup>1</sup>Slovak Hydrometeorological Institute, Poprad-Gánovce, 058 01, Slovakia

5 *Correspondence to:* Peter Hrabčák (peter.hrabcak@shmu.sk)

**Abstract.** Atmospheric ozone along with aerosols significantly affect the amount of ultraviolet solar radiation that reaches on the Earth's surface. Presented study is focused on the comparison of the optical depth of total ozone and atmospheric aerosols in the area of Poprad-Gánovce situated at the altitude of 706 meters above sea level, close to the highest peak of the Carpathian Mountains. Measurements of direct sun ultraviolet radiation are carried out here continuously since 1994 using the Brewer Ozone Spectrophotometer type MK IV. These measurements are used to calculate the total amount of atmospheric ozone and consequently its optical depth. Measurements can also be used to determine the optical depth of atmospheric aerosols using the Langley plot method. In this study, those two factors causing a significant reduction in the direct sun ultraviolet radiation to the Earth's surface are compared to each other. The study is showing results of measurements over 23 years, since 1994 to 2016. Values of optical depth are determined for wavelengths 306.3 nm, 310.1 nm, 313.5 nm, 316.8 nm and 320.1 nm. A statistically significant decrease in the total optical depth of the atmosphere was observed for all investigated wavelengths. Its main cause is the decrease of optical depth of aerosols. The study also presents comparison of the terrestrial and satellite data of total ozone and AOD. A very good match of satellite and terrestrial direct sun measurements of total ozone was found. The use of zenith sky measurements in combination with the direct sun measurements leads to the systematically higher values of total ozone. Comparison of the satellite and terrestrial AOD measurements in the UV range of the solar spectrum is mainly limited by the very low number of days for which AOD can be determined for satellite measurements. It has been found that AOD satellite data is higher than terrestrial in the long-term average.

### 1 Introduction

As it is known, anthropogenic changes in the amount of total ozone and atmospheric aerosols significantly affect the sun's UV radiation hitting the Earth's surface (De Bock et al., 2014; Czerwińska et al., 2016). Increased transmittance of UV radiation through the Earth's atmosphere obviously affects human health and natural ecosystems. Adverse effects have higher doses of UV radiation mainly on terrestrial plants exposed to it for a long time (Jansen et al., 1998). Effects of excessive doses of UV radiation on the human body can cause premature skin ageing, weakening of the immune system, damage of cells and DNA, which can then lead to skin cancer and other health problems (Greinert et al., 2015). Positive



effects of UV radiation are also known such as production of vitamin D in the skin. This vitamin is very necessary for the proper functioning of the human body (Kimlin and Schallhorn, 2004). The anthropogenic effect in the past has led to the increase of transmission of sun UV radiation through the Earth's atmosphere as the consequence of decrease in the total amount of ozone. Depletion of the global ozone layer began to emerge gradually in the 1980s and reached a maximum of about 5 % (relative to the 1964–1980 average) in the early 1990s. In the last few years, the weakening has been even lower, reaching about 3 % on average for the whole Earth (WMO, 2014). At mid-latitudes of the northern hemisphere (35° N–60° N), the ozone layer decreased by 3.5 % around the year 2010 (2008–2012). At the same time, for the mid-latitudes of the southern hemisphere (35° S–60° S) there was a decrease of up to 6 % (WMO, 2014).

On the other hand, the anthropogenic emission of aerosols into the atmosphere causes the reduction of sun UV radiation hitting on the Earth's surface, especially in the industrialized areas. At the beginning of the 1990s, it was found that in the non-industrialized areas of industrialized countries, solar UV-B radiation decreased since the industrial revolution by about 5–18 % as a result of air pollution (Liu et al., 1991). Even in highly polluted urban areas, anthropogenic aerosols can reduce UV radiation hitting on the Earth's surface by more than 50 % (Krotkov et al., 1998; Sellitto et al., 2006). In developed countries, the anthropogenic emission of aerosols is gradually reduced and in several places we see the decrease of optical depth of aerosols (AOD), (Kazadzis et al., 2007; Mishchenko and Geogdzhayev, 2007; Alpert et al., 2012; de Meij et al., 2012). Aerosols also have a significant impact on other physical and chemical processes ongoing in the atmosphere (Seinfeld and Pandis, 2006; Raghavendra Kumar et al., 2010). In particular, it affects the chemical composition of the troposphere, but in certain cases also the stratospheric ones, especially in the case of large volcanic eruptions or aircraft flights in the stratosphere (Finlayson and Pitts, 2000; Seinfeld and Pandis, 2006). They are able to reduce visibility (Lyamani et al., 2010) and in many cases have the significant impact on human health (WHO, 2006). The presence of aerosols in the atmosphere has also an impact on the Earth's energy balance in direct, semi-direct and indirect way (De Bock et al., 2010).

In direct way is meant scattering and absorption of shortwave and longwave radiation. Absorption of radiation then leads to the warming up of those parts of the atmosphere where the aerosols are found (especially the boundary layer of the atmosphere) and the higher temperature subsequently leading to the evaporation of the clouding layers. By the last sentence was briefly described semi-direct way resulting in the greater density of solar radiation hitting on the Earth's surface (Cazorla et al., 2009). Higher temperatures can also lead to a change of the temperature layers of the atmosphere, which subsequently affects the vertical and horizontal movements of air in the atmosphere. The indirect effect relates to the ability of aerosols to act as condensation nuclei or ice cores, which affects the microphysical and optical properties of clouds. This is a change of their radiation properties, a change of the properties of atmospheric precipitation and also changes the life of clouds. It is true that an increase in the number of cloudy condensation nuclei leads to an increase in the number of cloud drops and to a reduction in their size under given conditions of the water content in the atmosphere, which causes the growth of the albedo and the lifetime of the cloud (Lohmann and Feichter, 2005; Unger et al., 2009). For these reasons, anthropogenically emitted aerosol particles have a significant role to play in the ongoing global climate change and their impact on the radiation balance still has high uncertainties (IPCC, 2014, and references therein).



This study is focused mainly on the aerosols optical depth (AOD) obtained by Brewer's ozone spectrophotometer measurements and presents one of the possible methodological approaches to its calculation. AOD obtained results are compared with the influence of optical depth of the total atmospheric ozone on the reduction of sun UV radiation and satellite measurements, all for the area Poprad-Gánovce. Brewer allows to determine the optical depth in the UV range of the  
5 wavelengths 306.3 nm, 310.1 nm, 313.5 nm, 316.8 nm and 320.1 nm. A Langley plot method (LPM) was used to calculate the AOD. This is the traditional method used to calculate AOD using Brewer (Carvalho and Henriques, 2000; Kirchhoff et al., 2001; Silva and Kirchhoff 2004; Cheymol et al., 2006; Sellitto et al. 2006). This method requires stable atmospheric conditions to determine the extraterrestrial constant (ETC). In particular, there is required the low variability of total ozone and atmospheric aerosols over the day for which ETC is determined. It is also necessary to prevent cloud impact on direct  
10 solar radiation (DS) measurements and to ensure a sufficient range of zenith angles of individual DS measurements during the day that is required for the given method.

From the above reason this method is the best used in lower latitudes (especially in mountainous areas near the Tropic of Cancer and the Tropic of Capricorn) and has certain limitations in middle and especially higher latitudes (Nieke et al. 1999; Marengo 2007). This method of calculating the AOD has already been used in the past for an investigated area  
15 Poprad-Gánovce (Pribullová, 2002). Alternative method of calculating AOD has also been available since 2005 (Savastiouk and McElroy, 2005; Savastiouk, 2006; Kumharn et al., 2012). In this case, the AOD calculation algorithm is part of the main control program for Brewer. The main difference from previous method is that the ETCs for individual wavelengths are not determined by LPM method but they are obtained during calibrating the instrument, i.e. every 2 years. The disadvantage of both the first and the second method are neglected changes in the sensitivity of instrument in the shorter time intervals seeing  
20 that ETCs are fixed for longer period, e.g. 2 years.

## 2 Methods

### 2.1 Instrumentation

Brewer's Ozone Spectrophotometer (model MKIV) is a scientific instrument that works in the ultraviolet and visible range of the solar spectrum. Measurements of direct UV solar radiation are performed at selected wavelengths. It is possible to derive  
25 the total amount of ozone and sulfur dioxide based on the different absorption of radiation after pass through the atmosphere. This principle of measurement using passive atmospheric differential spectroscopy is known as so called DOAS method (Differential optical absorption spectroscopy). The instrument uses its optical system to decompose solar radiation hitting on the Earth's surface and selects predetermined wavelengths with strong and weaker absorption of O<sub>3</sub> and SO<sub>2</sub> from the ultraviolet part of its spectrum. The total amount of O<sub>3</sub> and SO<sub>2</sub> in the vertical column of the atmosphere between its upper  
30 boundary and the Earth's surface is possible to determine by following a comparative analysis in the mathematical model describing transmission of radiation in the atmosphere. Measurements of direct solar radiation are also used to calculate AOD. In the ultraviolet area of the solar spectrum it is feasible for wavelengths 306.3 nm, 310.1 nm, 313.5 nm, 316.8 nm



and 320.1 nm. The instrument's accuracy for determining the wavelength is  $0.006 \pm 0.002$  nm per one step (Sci-Tec, 1999). Since the beginning of measurements (18 August 1993) device no. 097 undergoing regular 2-year calibrations and daily tests using internal lamps (mercury and standard lamp). Calibration is provided by International Ozone Services (IOS). The instrument is calibrated according to the global reference group Brewer Triad (World Meteorological Organization standards) maintained at Environment Canada through travel reference instrument no. 017.

## 2.2 The place of experiment

The Brewer Ozone Spectrophotometer is placed on the roof of the building of Upper Air and Radiation Centre of the Slovak Hydrometeorological Institute (SHMI) in Gánovce near the town of Poprad. Its coordinates are  $49.03^\circ$  N and  $20.32^\circ$  E and the altitude is 706 meters above sea level. The content of aerosols in the air, whether the total quantity or species composition, determines on the one hand local sources and, on the other hand, atmospheric flow which can transfer the certain air mass along with aerosols for several thousand kilometers. In rare cases, it can also be e.g. the transport of Saharan dust from Africa. In 2016, Saharan dust was present over the Slovak Republic for at least twenty days (Hrabčák, 2016). Major local resources include solid fuel combustion products in the surrounding villages and agriculture. There is frequent wearing of bare dry soil or plant products by wind because the site is relatively windy. The proximity of the town of Poprad (approx. 1.5 km) with about 53 000 inhabitants and various industrial activities also plays its role.

## 2.3 Calculation of the optical depth of total ozone

Measured total ozone values obtained by direct sun (DS) measurement through Brewer we used for the calculation of the optical depth of total ozone. The DS measurement is performed only at a relative optical mass less than 4 and takes about 2.5 minutes. During this time, the density of the solar radiation for each of the five wavelengths is measured five times. Thus, a single DS measurement gives five total ozone values in Dobson units (DU) from which average and standard deviation are then calculated. Only DS measurements that meet the standard deviation criterion ( $STDEV \leq 2.5$  DU) are selected for further data analysis. Total ozone was calculated using the software Brewer Spectrophotometer B Data Files Analysis Program v. 5.0 by Martin Stanek (<http://www.o3soft.eu/o3brewer.html>). Optical depth was calculated for each accepted total ozone value. Calculation is evident from the following Eq. (1):

$$\tau_{\lambda, O_3} = \Omega_{O_3} \alpha(\lambda, T) = \Omega_{O_3} \sigma(\lambda, T) n, \quad (1)$$

where  $\tau_{\lambda, O_3}$  is optical depth of the total ozone,  $\Omega_{O_3}$  is thickness of total ozone in Dobson units,  $\alpha(\lambda, T)$  is the absorption coefficient for ozone,  $\sigma(\lambda, T)$  is effective absorption cross-section of the ozone molecule (it is used to quantify it with respect to  $1 \text{ cm}^2$ ), and  $n$  is the number of molecules in a volume determined by 1 DU and  $1 \text{ cm}^2$ , for  $O_3$  it is a constant with value  $n = 2.69 \cdot 10^{16}$  (Schwartz and Warneck, 1995). Effective absorption cross-section of the ozone molecule was obtained on the basis of measurements of the University of Bremen (<http://www.iup.physik.uni-bremen.de/gruppen/molspec/databases/index.html>; Gorshelev et al., 2014; Serdyuchenko et al., 2014). A very important fact



is the dependence of the effective absorption cross-section on the temperature. It is used to using so called an effective temperature characteristic for given gas. For ozone measurements using Brewer, the average standard effective temperature - 45 °C (228.15 K) is defined (Redondas et al., 2014).

#### 2.4 Calculation of the aerosols optical depth

5 For calculation of AOD, the Beer-Bouguer-Lamberts Law had to be applied:

$$S_{\lambda} = S_{0,\lambda} e^{-m_r \tau_{\lambda}} = S_{0,\lambda} e^{-\mu_{O_3} \tau_{\lambda,O_3} - \mu_r \tau_{\lambda,r} - \mu_a \tau_{\lambda,a}} = S_{0,\lambda} e^{-\mu_{O_3} \alpha(\lambda,T) \Omega_{O_3} - \mu_r \frac{\beta(\lambda)P}{P_{std}} - \mu_a \tau_{\lambda,a}}, \quad (2)$$

where  $S_{\lambda}$  is density of solar radiation flux for selected wavelength and is expressed by the number of photons per unit of time on the Earth's surface,  $S_{0,\lambda}$  is density of solar radiation flux for the selected wavelength and is expressed by the number of photons per unit of time above the Earth's atmosphere (extraterrestrial constant - ETC),  $\tau_{\lambda}$  is total optical depth of the atmosphere,  $\tau_{\lambda,O_3}$  is optical depth for ozone,  $\tau_{\lambda,r}$  is optical depth for Rayleigh scattering,  $\tau_{\lambda,a}$  is optical depth for aerosols,  $m_r$  is air mass factor for the atmosphere as a whole,  $\mu_{O_3}$  is air mass factor for the ozone layer,  $\mu_r$  is air mass factor for Rayleigh scattering,  $\mu_a$  is air mass factor of aerosols,  $\alpha(\lambda,T)$  is absorption coefficient for ozone,  $\Omega_{O_3}$  is total amount of ozone in Dobson units,  $\beta(\lambda)$  is normalized optical depth for Rayleigh scattering (for standard atmospheric air pressure and vertical column),  $P$  is atmospheric air pressure at the site of observation (multiannual average) and  $P_{std}$  is standard atmospheric air pressure (101 325 Pa). Sulfur dioxide contribution was neglected due to its low impact and also due to its inaccurate determination.

The value  $S_{\lambda}$  was obtained by adjusting the raw data (Raw counts). It is important to keep up the sequence of following steps. Raw counts stored in the B-file were converted to count rates in the first step, deadtime compensation was applied in the second step, then there was correction for the temperature dependence, and finally, in the fourth step, a correction was applied with respect to neutral density (ND) filter used. These filters are automatically selected by Brewer based on the current density of solar radiation flux. ND of filters and wavelengths is five so 25 attenuation values in total are needed. Attenuation values of given filters are determined during calibration of the instrument. Five initial values  $S_{\lambda}$  are obtained from one DS measurement and the arithmetic average is then calculated. The given average is used as input in Eq. (2). ETC  $S_{0,\lambda}$  was determined using the Langley plot method (LPM). Langley plot method uses multiple measurements of direct solar radiation at various sun zeniths in the sky. Its basic principle is as follows: the above Eq. (2) is adjusted by applying the natural logarithm:

$$\ln(S_{\lambda}) = \ln(S_{0,\lambda}) - m_r \tau_{\lambda}. \quad (3)$$

For each DS measurement there is one equation available, while known are  $m_r$  and  $\ln(S_{\lambda})$ , and unknown are  $\ln(S_{0,\lambda})$  and  $\tau_{\lambda}$ . Using multiple measurements of the various zenith angles of the Sun, the same number of equations as the number of measurements is obtained. Theoretically, it is possible to determine unknown from two measurements, but for practical purposes it is appropriate to obtain the highest possible number of measurements, it guarantees a higher accuracy of the result. It is essential to linearly interpolate the obtained dependence of natural logarithm of the density of solar radiation flux



$\ln(S_\lambda)$  on total air mass factor of the atmosphere  $m_T$ , using the method of the smallest squares. The slope of the obtained line  $a$  (from line equation  $y = ax + b$ ) is equal to  $\tau_\lambda$ . The natural logarithm ETC  $\ln(S_{0,\lambda})$  is obtained when  $x$  (in the line equation) is equal to zero ( $x$  represents  $m_T$ ). ETC for a given wavelength is valid for entire calibration period, i.e. 2 years. Its determination is carried out in two steps. In the first step, in particular calibration period are selected days for which ETCs
   
5 will be calculated. These selected days must comply the following criteria:

1. Only those DS measurements are accepted for which applies the condition: variation coefficient calculated from five initial values is less than 10 % for all investigated wavelengths.
- 10 2. Number of DS measurements is at least 7.
3. Standard deviation of all measured total ozone values is less than 2.5 on the given day.
4. Standard deviation of all measured AOD values is less than 0.07 on the given day.
- 15 5. Difference between maximum and minimum total relative atmospheric mass of the atmosphere for DS measurements is greater than 1.
6. Determination coefficient for linear interpolation is greater than 0.98.

20

In the second step, following criterion is applied to all ETCs set in the given calibration period:

$$\frac{|ETC - \text{AVERAGE}(ETCs)|}{\text{STDEV}(ETCs)} < 1.5, \quad (4)$$

where AVERAGE (ETCs) is the average of the specified ETCs and STDEV (ETCs) is their standard deviation. From the ETCs that met this criterion, the average is calculated. This average is valid for entire calibration period. It is important to
   
25 note that criteria 4 and 5 have been applied only if there were already available so called initial values AOD. To calculate initial values AOD, only criteria 1., 2., 3. and 6. were applied in the first step. Criterion 1. was applied to all DS measurements, in addition to ETCs calculation, of which the standard deviation for initial values AOD in 4. criterion was determined. ETC changes over the year around its mean value with respect to the distance of Earth from the Sun. Its correction was performed according to the Guide for meteorological instruments and methods of observation (WMO, 2008).

30 Air mass factor (AMF) was calculated as:

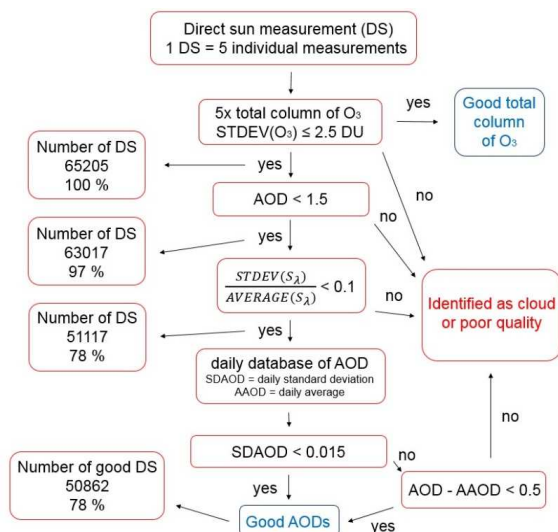
$$\text{AMF} = \sec\left[\arcsin\left(\frac{R_E}{R_E+h} \sin \vartheta\right)\right], \quad (5)$$



where  $R_E$  is Earth's radius in the place of measurement (6370 km),  $h$  is characteristic altitude (2 km for aerosols, 5 km for atmosphere as a whole and Rayleigh scattering, 22 km for ozone) and  $\vartheta$  is zenith angle of the Sun. The value  $\beta(\lambda)$  was calculated according to Bodhaine et al. (1999) and is given as:

$$\beta(\lambda) = 0,002152 \frac{1,0455996 - 341,29061 \lambda^{-2} - 0,9023085 \lambda^2}{1 + 0,0027059889 \lambda^{-2} - 85,968563 \lambda^2} \quad (6)$$

- 5 All final values AOD have passed the cloud screening process, which is schematically illustrated in Fig. 1. Prior to the cloud screening process, all negative AOD values were removed. The number of DS measurements that entered the cloud screening process is 65 205. After applying all of the above criteria, we received 50 862 measurements representing 78 % of number of measurements at input.



- 10 **Figure 1: Schematic illustration of the cloud screening. On the left is listed the number of DS measurements that meet the relevant criterion.**

When calculating individual characteristics of optical depth of total ozone and AOD was progressed as follow: Daily averages are calculated as arithmetic average of all values of a given day (from at least one value). Monthly averages are calculated as arithmetic average of those days for which the average daily value is available. Annual averages are calculated as arithmetic average of individual monthly values. The linear trend was calculated by linear regression through the smallest square method. Autocorrelation was not confirmed, therefore a linear trend could be established. Uncertainty of linear trend is defined by standard deviation ( $\pm \sigma$ ). Size of linear trend and standard deviation were set for a ten year period. The seasonal cycle was removed using annual averages. When calculating total ozone using direct sun (DS) and zenith sky (ZS)

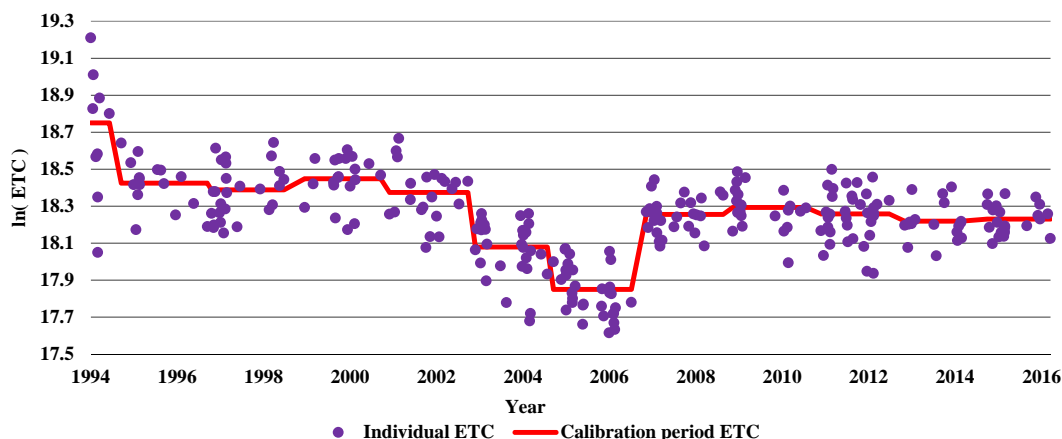


measurements is true that if there is at least 1 DS measurement available on the given day, it always takes precedence over ZS measurements.

### 3 Results and discussion

#### 3.1 ETC

5 In the previous section, ETCs calculation methodology was also described in more detail for individual wavelengths. Strict conditions for choosing the right days to determine and other criteria mentioned eliminate non-representative values. Despite the strict conditions, obtained ETCs show some variability within calibration period. This variability is observed for all investigated wavelengths. In the long-term average is the highest for the shortest wavelength. Variation coefficient for it is up to 16.8 %. On the contrary, the lowest variability is typical for the longest wavelength. In this case, variation coefficient is  
10 13.6 %. The above mentioned variability can be seen in Fig. 2, where ETCs (their natural logarithm) values are shown for each day, for the longest wavelength 320.1 nm. A graph also shows ETCs values which characterize entire two-year calibration period. For their determination, 25 ETCs were used on average. In other words, strict conditions met on average only 25 days in a two-year calibration period representing 3.4 %. If conditions were less strict, days for which ETC could be set would be more. On the other hand, the scatter of established ETCs would be larger and this would negatively affect the  
15 required accuracy. Therefore, chosen criteria are optimal compromise. The uncertainty of ETC determination directly affects to the resulting values AOD. The main cause of this inaccuracy are probably the weather effects which significantly eliminate number of days that are appropriate for determining the ETC. Other factors may include instrument instability. Fact that the device is not calibrated to stray-light effects also plays the certain role.



20 Figure 2: Evolution of ETC values for wavelength 320.1 nm during the 12 calibration periods, 1994–2016.





As can be seen in Fig. 2, during reference period of 23 years, ETC value for the observed wavelength does not remain constant. Some changes occurred in all five examined wavelengths. 12 ETCs values were determined for each wavelength, one for each calibration period. The greatest instability was observed for the shortest wavelength, the variation coefficient is 21.9 %. On the contrary, the smallest instability was observed in wavelength 313.5 nm, the variation coefficient is 18.9 %. In Fig. 2 it can be noticed that the more significant change in the ETC value in the case of the longest wavelength occurred altogether 4 times. The first change occurred between the 1st and 2nd calibration period. This change has no specific explanation. It is likely to be related to the instability of ETCs during the 1st calibration period. This instability may have been caused by that calibration period was shorter (resulting in fewer days to determine ETC) and also that the instrument was new. Three more changes occurred between the 5th, 6th, 7th and 8th calibration period. They were caused by instrumental problems. For this reason, the Secondary power supply board had to be replaced in January 2005. In February 2007, micrometer was replaced and during calibration in May 2007 optical filter no. 3 was replaced and also BM-E80 high-frequency source was repaired.

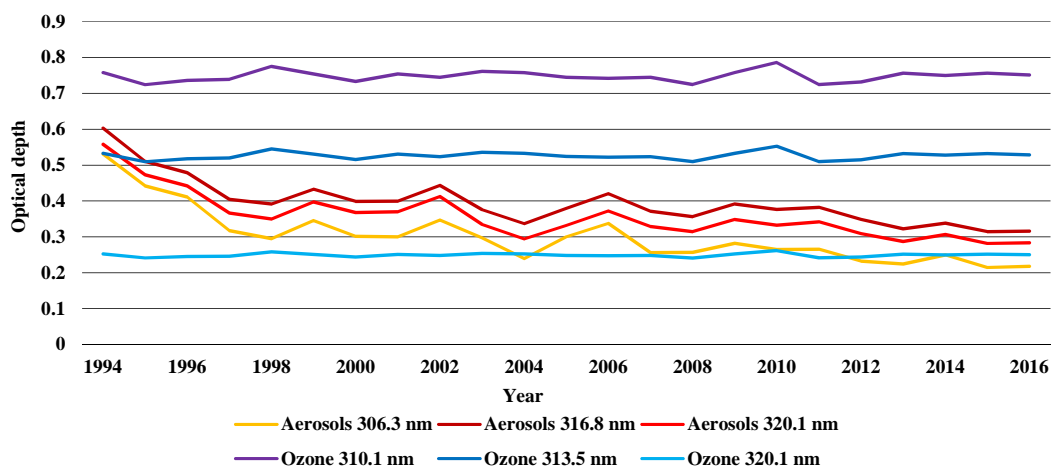
### 3.2 Optical depth of total ozone and AOD

Total ozone measurements are available from Brewer for Poprad-Gánovce station only since 1994. Using ground measurements from the nearby station in Hradec Králové and satellite data, it was possible to derive ozone status already since 1962. Based on the available data it was found that the amount of total ozone above the area Poprad-Gánovce reached a minimum with respect to the 5-year moving average in 1994 with a value of 320 DU, what is 6.5 % less than the long-term average of 1964–1980. In the last five years (2012–2016), average value was 330 DU, what is 3.6 % less than the long-term average of 1964–1980. Annual averages of total amount of ozone from Brewer measurements using direct sun (DS) and zenith sky (ZS) measurements show since 1994 to 2016 a rising trend of  $2.6 \pm 2.3$  DU for 10 years. If optical depth of total ozone is determined only from DS measurements, than trend is  $0.8 \pm 2.2$  DU for 10 years. For this reason, rising trend of the optical depth of total ozone for monitored wavelengths is also statistically insignificant. For wavelength 306.3 nm, trend is  $0.003 \pm 0.009$  for 10 years and for wavelength 320.1 nm trend is  $0.001 \pm 0.002$  for 10 years.

In Fig. 3, it is possible to see comparison of annual averages of the optical depth of total ozone and aerosols for selected wavelengths. Already at first sight is evident that AOD in contrast to the optical depth of total ozone, shows obvious decline over reference period. For wavelength 306.3 nm, trend is  $-0.09 \pm 0.01$  for 10 years and for the wavelength 320.1 nm, the trend is  $-0.08 \pm 0.01$  for 10 years. Considering mentioned facts, it can be concluded that transmittance of the atmosphere in studied wavelengths has increased in the Poprad-Gánovce area over the past 23 years. Total optical depth of the atmosphere for wavelength 306.3 nm has trend of  $-0.09 \pm 0.02$  for 10 years and for wavelength 320.1 nm, trend is  $-0.08 \pm 0.01$  for 10 years. This trend is caused mainly by decrease of AOD. The following Fig. 4 shows annual averages of AOD for wavelength 320.1 nm together with the uncertainty of their determination. Annual averages of AOD were calculated as standard, i.e. through the average value ETC. The lower limit of uncertainty was calculated using average value ETC from which its standard deviation has been deducted in the given calibration period. The upper limit of uncertainty was



determined analogously. The broadest uncertainty range occurs in 1994, which is associated with large uncertainty of ETC determination in the first calibration period. Width of the uncertainty interval depends mainly on the appropriate weather conditions in the given calibration period and also on stability and homogeneity of the measurements during the days when it was possible to determine ETC.



5

Figure 3: Comparison of average annual optical depth for selected wavelengths, ozone and aerosols, 1994–2016.

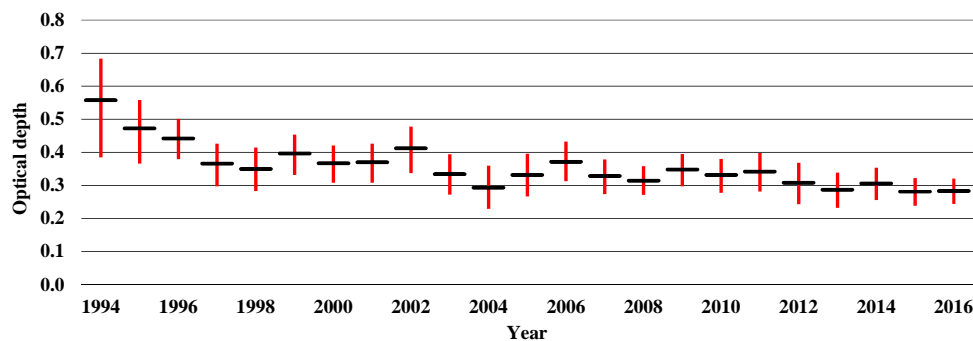


Figure 4: Annual averages of AOD and their uncertainty for wavelength 320.1 nm, 1994–2016.

10

Fig. 5 presents a comparison of the multi-year averages of the optical depth of ozone, optical depth of Rayleigh scattering and AOD for all 5 examined wavelengths. It can be seen that ozone is dominant only for the shortest wavelength. It's exactly the opposite for the pair of the longest wavelengths and ozone has the smallest influence among the examined factors.



Rayleigh scattering has a dominant position at weakening of direct solar radiation for all wavelengths except the shortest. In the case of AOD, it is not observed unique dependence of its size from wavelength. The highest value has AOD for a wavelength 316.8 nm, this is 0.4. On the contrary, the smallest value has AOD for wavelength 306.3 nm, it is 0.3. In the same way, the study Pribullová (2002) does not give a unique dependence of AOD size from wavelength. The lowest AOD indicates in the case of shortest wavelength, so here is the match with our result. A match can not be seen in the case of the highest AOD value which it presents for a wavelength 310.1 nm.

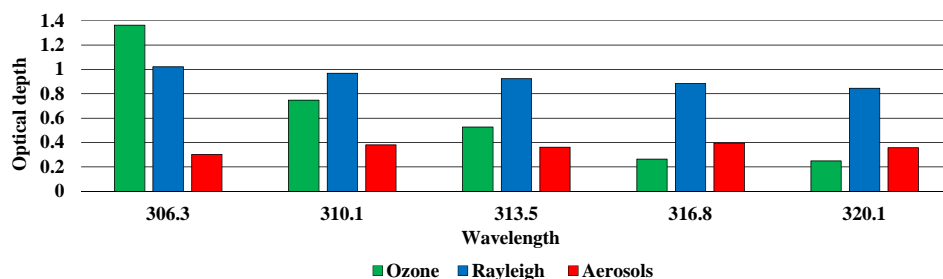
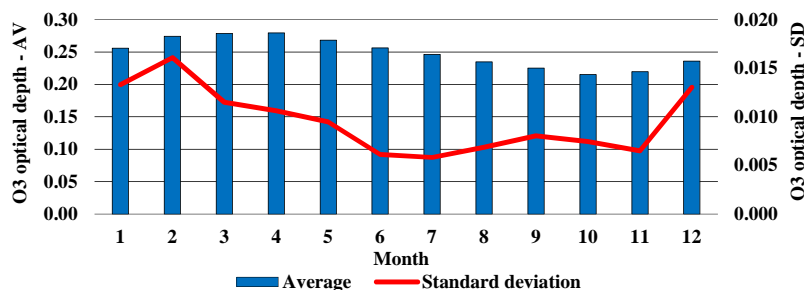


Figure 5: Comparison of long-term averages of optical depth of total ozone, optical depth of Rayleigh scattering and AOD, 1994–2016.

10

Fig. 6 illustrates the annual optical ozone depth and its variability for individual months, all for a wavelength 320.1 nm. Optical depth reaches maximum in March and April with a value of 0.279 and minimum in October with a value of 0.215. The highest variability is in February and the smallest variability is in July. In each month of the year, the variability is significantly smaller than the average. The maximum coefficient of variation has February with a value of 5.9 %.



15

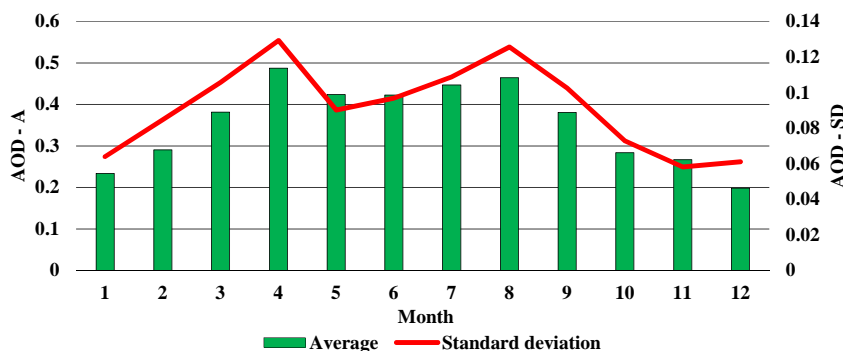
Figure 6: Average monthly characteristics of optical depth of total ozone for wavelength 320.1 nm, 1994–2016.

Fig. 7 presents the same characteristics as Fig. 6 but in this case for AOD. Annual flow of monthly averages is characterized by two peaks. The primary peak, that is annual maximum, it occurs in April with a value of 0.49. Secondary peak occurs in August with a value of 0.46. The minimum is in December with a value of 0.2. The variability is also characteristic by

20



two-peak annual flow. The primary and secondary peaks are equal in the same months as for average. Annual minimum is in November. Variation coefficient is significantly higher than the ozone. The minimum is May with a value of 19.4 %. The maximum is December with a value of up to 27.1 %.



5 Figure 7: Average monthly AOD characteristics for wavelength 320.1 nm, 1994–2016.

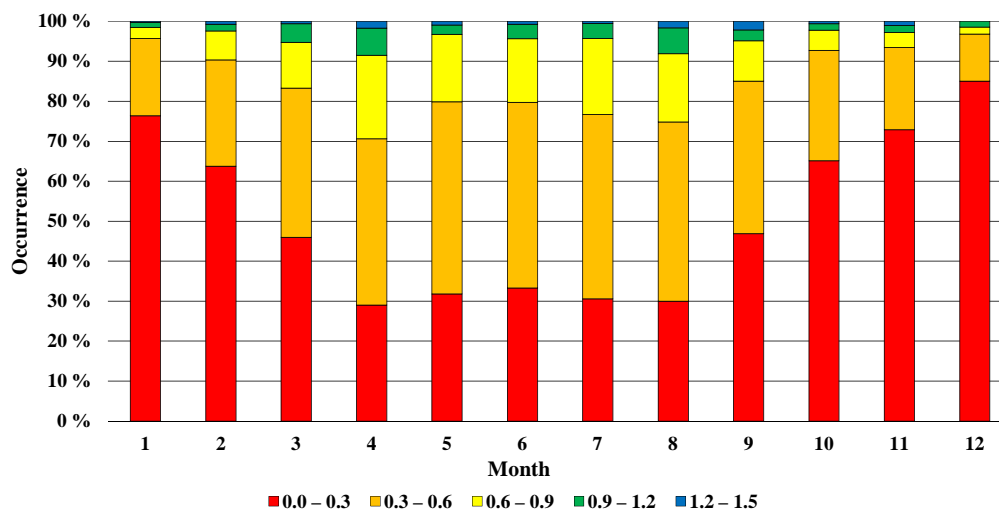


Figure 8: Relative distribution of daily average AOD values for wavelength 320.1 nm, 1994–2016.

10 In Fig. 8, it is possible to see relative distribution of daily AOD averages for individual months of the year over reference period 1994–2016. It is important to note that were considered only the days for which the AOD could be determined. In December, there is the highest percentage of days with AOD in the range of 0 to 0.3, particular it is up to 85 %. In the



months from April to August dominate days with daily average of AOD in the range from 0.3 to 0.6. In the remaining months of the year dominate days with a daily average of AOD in the range from 0 to 0.3. AOD above 0.6 is the most common in April, i.e. 29 % days. The smallest representation has such days in December, it is only 3 %.

### 3.3 Comparison of the terrestrial and satellite measurements

5 The basic difference between terrestrial measurements from Brewer and satellite measurements via Ozone Monitoring Instrument (OMI) located on the AURA satellite consists of their temporal and spatial resolution. If the weather conditions allow it, then DS measurements by Brewer are carried out every half hour, on the other hand satellite measurement of total ozone (DOAS method) and AOD is performed above the given location only once a day. Data from Brewer characterize scored specific place, on the other hand, the resolution of satellite data (Veefkind, 2012); (Stein-Zweers and Veefkinf, 2012)  
10 is  $0.25^\circ$  (this corresponds to the square with dimensions of 28 x 28 km). Despite these differences, the comparison of daily average of total ozone and AOD were compared from 2005 to 2016. From daily averages of total ozone were determined monthly averages and consequently also annual averages.

In Fig. 9 is illustrated comparison of the annual averages of total ozone. Specifically it was the comparison of values obtained from satellite with values obtained from Brewer, with two calculation methods have been distinguished in  
15 the case of Brewer. The first uses DS and ZS measurements, the second uses only DS measurement. Very good match is observed between satellite measurements and DS Brewer measurements. Average difference have reached - 0.2 DU during monitored period of 12 years. The maximum difference was 2.1 in 2008 and the minimum difference was - 2.7 in 2014. Data obtained from Brewer using a combination of DS and ZS measurements show higher values for annual averages compared to DS measurements as well as compared to satellite data. In the first case, the average annual difference is 3.7 DU and in the  
20 other case is 3.9 DU. Such a significant difference is caused by inconsistent methodology for the calculation of total ozone through ZS measurements. It can be said that this is probably the systematic error.

Fig. 10 illustrates comparison of the daily averages AOD from satellite and terrestrial measurements for a wavelength 320.1 nm. The instrument OMI determines AOD in sun UV spectrum for wavelengths 342.5 nm and 388 nm. AOD for a wavelength 320.1 nm was also calculated using an Ångström exponent describing the change of AOD for  
25 measured pair of wavelengths. For monitored 12 year period it was possible to compare each other for only 223 days. This is due a very few days with a specified AOD through satellite measurements. In this case, AOD was determined for only 5.7 % of days, furthermore only AOD values were smaller than 1.5 were taken into the further analysis. The correlation coefficient has reached the value of 0.51 in comparison with each other what represents a strong positive correlation. Total average AOD from all observed days is for terrestrial measurements of 0.26 and for satellite measurements of 0.38. It is  
30 evident that satellite data is higher than terrestrial in long-term average. The cause is likely in limited cloud screening capabilities so far as the instrument OMI determines AOD for an area of up to 784 km<sup>2</sup>. Therefore, sometimes cloudiness is also included among aerosols.

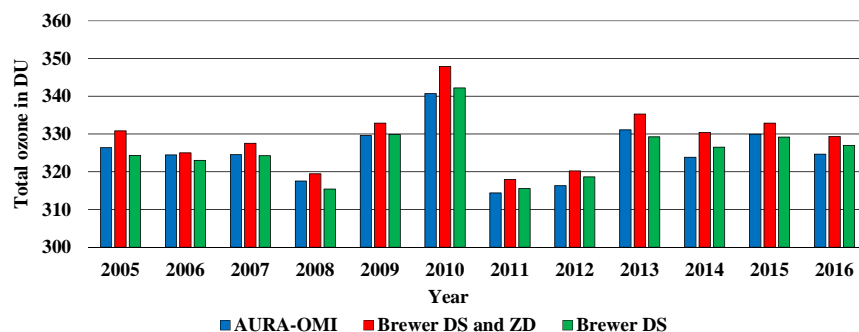
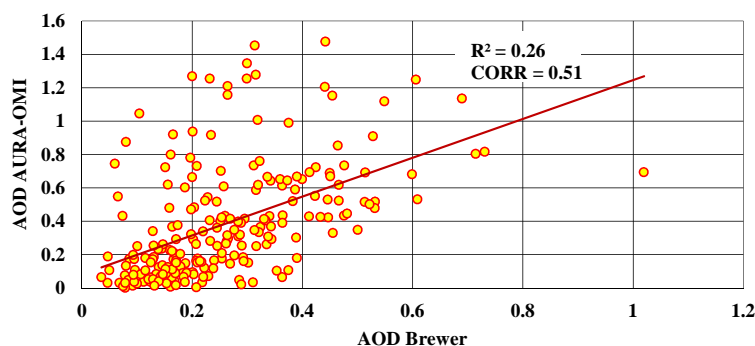


Figure 9: Comparison of annual averages of total ozone obtained by satellite and terrestrial measurements, 2005–2016.



5 Figure 10: Comparison of daily averages AOD for wavelength 320.1 nm obtained from Brewer and satellite measurements, 2005–2016.

#### 4 Conclusions

Optical depth of the total ozone and aerosols was determined using measurements of Brewer's ozone spectrophotometer in Gánovce near Poprad. AOD was calculated through ETCs obtained using the Langley plot method. Analyzed data of direct  
10 sunlight was available since 1994 to 2016 so it is a period of 23 years of measurements. In the 1990s, the ETCs were not determined during the calibrations and for this reason the LPM method is the only possible method to determine AOD for a whole range of measurements. ETCs used in this study have been determined for a 2-year calibration period. Using such a long time period has its advantage and, on the other hand, its disadvantage. The advantage lies in the fact that ETC determined as the average from a larger number of days prevents random impact of fluctuations which do not have a specific  
15 explanation. Disadvantage is suppression of the weather effects (especially the change of temperature) and instrumental



changes at time intervals of less than two years. In addition to the methodology of ETCs determination, the cloud screening also affects the AOD values. AOD would be significantly higher without using cloud screening. Cloud screening used in this study is relatively simple and therefore it can be argued that real AOD is relatively lower. This is the case especially of presented monthly and annual averages. In the future is planned to improve the cloud screening methodology and thanks to

5 that it will be possible to obtain more representative AOD values.

Obtained results clearly indicate a decrease in annual average values of the total optical depth of atmosphere for observed wavelengths since 1994 to 2016. It is observed a slightly increasing trend of total ozone which is expressed in only statistically insignificant increase of optical depth of total ozone. This insignificant increase influences trend of the total optical depth of atmosphere only minimal. The main reason of decrease in the total optical depth of atmosphere is

10 statistically significant decrease of AOD. It follows that transmittance of the atmosphere in UV area of the spectrum from 306.3 nm to 320.1 nm has increased in Poprad-Gánovce.

From comparison of the terrestrial measurements of total ozone from Brewer through DS measurements and satellite measurements through the OMI results in a very good match. Combined methodology using DS and ZS measurements clearly shows higher values than satellite and terrestrial DS measurements. The reason for this is probably the

15 systematic error of the ozone determination using ZS measurements. Limit factor in comparing the terrestrial and satellite AOD measurements is the very low number of days for which was determined AOD through satellite. Comparison of daily averages AOD suggests that satellite data are higher than terrestrial in the long-term average, for the reason of limited cloud screening options for satellite data, and therefore the cloud effect can not be sufficiently eliminated.

20 *Data availability.* Data used in the research and presented in this paper can be obtained in agreement with author of the article. It is recommended to ask him by e-mail.

*Competing interests.* Author declares that he has none conflict of interests.

25 *Acknowledgements.* Author of the article thanks the Slovak Hydrometeorological Institute for providing data. Further thanks to the Faculty of Mathematics, Physics and Informatics of Comenius University in Bratislava for the possibility of an external PhD. study in the field of meteorology and climatology. Many thanks also belongs to the organizing team of International Conference Quadrennial Ozone Symposium held in Edinburgh 4.–9. September 2016, also for providing financial support.

### 30 **References**

Alpert, P., Shvainshtein, O., and Kishcha, P.: AOD trends over megacities based on space monitoring using MODIS and MISR, *Am. J. Clim. Change*, 12, 117–131, doi:10.4236/ajcc.2012.13010, 2012.



- Bodhaine, B. A., Wood, N. B., Dutton, E. G., and Slusser, J. R.: On Rayleigh Optical Depth Calculations, *J. Atmos. Oceanic Technol.*, 16, 1854–1861, 1999.
- Carvalho, F., and Henriques, D.: Use of Brewer ozone spectrophotometer for aerosol optical depth measurements on ultraviolet region, *Adv. Space Res.*, 25, 997–1006, 2000.
- 5 Cazorla, A., Shields, J. E., Karr, M. E., Olmo, F. J., Burden, A., and Alados-Arboledas, L.: Technical Note: Determination of aerosol optical properties by a calibrated sky imager, *Atmos. Chem. Phys.*, 9, 6417–6427, doi:10.5194/acp-9-6417-2009, 2009.
- Cheymol, A., De Backer, H., Josefsson, W., and Stubi, R.: Comparison and validation of the aerosol optical depth obtained with the Langley plot method in the UV-B from Brewer Ozone Spectrophotometer measurements, *J. Geophys. Res.*, 10 111, D16202, doi:10.1029/2006JD007131, 2006.
- Czerwińska, A. E., Krzyściński, J. W., Jarosławski, J., and Posyński, M.: Effects of urban agglomeration on surface-UV doses: a comparison of Brewer measurements in Warsaw and Belsk, Poland, for the period 2013–2015, *Atmos. Chem. Phys.*, 16, 13641–13651, doi:10.5194/acp-16-13641-2016, 2016.
- De Bock, V., De Backer, H., Mangold, A., and Delcloo, A.: Aerosol Optical Depth measurements at 340 nm with a Brewer spectrophotometer and comparison with Cimel sunphotometer observations at Uccle, Belgium, *Atmos. Meas. Tech.*, 3, 1577–1588, doi:10.5194/amt-3-1577-2010, 2010.
- 15 De Bock, V., De Backer, H., Van Malderen, R., Mangold, A., and Delcloo, A.: Relations between erythemal UV dose, global solar radiation, total ozone column and aerosol optical depth at Uccle, Belgium, *Atmos. Chem. Phys.*, 14, 12251–12270, doi:10.5194/acp-14-12251-2014, 2014.
- 20 de Meij, A., Pozzer, A., and Lelieveld, J.: Trend analysis in aerosol optical depths and pollutant emission estimates between 2000 and 2009, *Atmos. Environ.*, 51, 75–85, doi:10.1016/j.atmosenv.2012.01.059, 2012.
- Finlayson-Pitts, B. J., Pitts, J. N.: *Chemistry of the upper and lower atmosphere: theory, experiments, and applications*, Academic Press, San Diego, USA, 2000.
- Gorshchev, V., Serdyuchenko, A., Weber, M., Chehade, W., and Burrows, J. P.: High spectral resolution ozone absorption cross-sections – Part 1: Measurements, data analysis and comparison with previous measurements around 293 K, *Atmos. Meas. Tech.*, 7, 609–624, 2014.
- 25 Greinert, R., de Vries, E., Erdmann, F., Espina, C., Auvinen, A., Kesminiene, A., and Schuz, J.: *European Code against Cancer 4th edition: Ultraviolet radiation and cancer*, *Cancer Epidem. Biomar.*, 39, S75–S83, 2015.
- Hrabčák, P.: Saharan dust over Slovakia, *Meteorological Journal*, 19/2, 83–91, 2016.
- 30 IPCC: *Climate change 2013: the physical science basis. Working Group I contribution to the Fifth Assessment Report of the Intergovernmental Panel on Climate Change*, Tech. rep., Intergovernmental Panel on Climate Change, 2014.
- Jansen, M. A., Gaba, V., and Greenberg, B. M.: Higher plants and UV-B radiation: balancing damage, repair and acclimation, *Trends in plant science*, 3(4), 131–135, 1998.





- Kazadzis, S., Bais, A., Kouremeti, N., Gerasopoulos, E., Garane, K., Blumthaler, M., Schallhart, B., and Cede, A.: Direct spectral measurements with a Brewer spectroradiometer: Absolute calibration and aerosol optical depth retrieval, *Appl. Opt.*, 44, 1681–1690, 2005.
- Kazadzis, S., Bais, A., Amiridis, V., Balis, D., Meleti, C., Kouremeti, N., and Tzoumaka, P.: Nine years of UV aerosol optical depth measurements at Thessaloniki, Greece, *Atmospheric Chemistry and Physics*, 7(8), 2091–2101, 2007.
- 5 Kimlin, M. G., and Schallhorn, K. A.: Estimations of the human ‘vitamin D’UV exposure in the USA, *Photochemical & Photobiological Sciences*, 3(11-12), 1067–1070, 2004.
- Krotkov, N. A., Bhartia, P. K., Herman, J. R., Fioletov, V., and Kerr, J.: Satellite estimation of spectral surface UV irradiance in the presence of tropospheric aerosols 1. Cloud-free case, *J. Geophys. Res.*, 103 (D8), 8779–8793, 1998.
- 10 Kumharn, W., Rimmer, J. S., Smedley, A. R. D., Ying, Y. T., and Webb, A. R.: Aerosol Optical Depth and the Global Brewer Network: A Study Using U.K. - and Malaysia-Based Brewer Spectrophotometers, *J. Atmos. Oceanic Technol.*, 29, 857–866, 2012.
- Kirchhoff, V. W. J. H., Silva, A. A., Costa, C. A., Lem, N. P., Pavao, H. G., and Zaratti, F.: UV-B optical thickness observations of the atmosphere, *J. Geophys. Res.*, 106, 2963–2973, 2001.
- 15 Liu, S. C., McKeen, S. A., and Madronich, S.: Effect of anthropogenic aerosols on biologically active ultraviolet radiation, *Geophys. Res. Lett.*, 18, 2265–2268, 1991.
- Lohmann, U. and Feichter, J.: Global indirect aerosol effects: a review, *Atmos. Chem. Phys.*, 5, 715–737, doi:10.5194/acp-5-715-2005, 2005.
- 20 Lyamani, H., Olmo, F. J., and Alados-Arboledas, L.: Physical and optical properties of aerosols over an urban location in Spain: seasonal and diurnal variability, *Atmos. Chem. Phys.*, 10, 239–254, doi:10.5194/acp-10-239-2010, 2010.
- Marenco, F.: On Langley plots in the presence of a systematic diurnal aerosol cycle centered at noon: A comment on recently proposed methodologies, *J. Geophys. Res.*, 112, D06205, doi:10.1029/2006JD007248, 2007.
- Mishchenko, M. I. and Geogdzhayev, I. V.: Satellite remote sensing reveals regional tropospheric aerosol trends, *Opt. Express*, 15, 7423–7438, doi:10.364/OE.15.007423, 2007.
- 25 Nieke, J., Pflug, B., and Zimmermann, G.: An aureolecorrected Langley-plot method developed for the calibration of HiRES grating spectrometers, *J. Atmos. Sol. Terr. Phys.*, 61, 739–744, 1999.
- Pribullová, A.: Spectral UV aerosol optical thickness determined from the Poprad-Gánovce Brewer spectrophotometer observations, *Contributions to Geophysics and Geodesy*, 32/3, 291–307, 2002.
- 30 Raghavendra Kumar, K., Narasimhulu, K., Balakrishnaiah, G., Suresh Kumar Reddy, B., Rama Gopal, K., Reddy, R. R., Satheesh, S. K., Krishna Moorthy, K., and Suresh Babu, S.: A study on the variations of optical and physical properties of aerosols over a tropical semi-arid station during grassland fire, *Atmos. Res.*, 95, 77–87, doi:10.1016/j.atmosres.2009.08.012, 2010.



- Redondas, A., Evans, R., Stuebi, R., Köhler, U., and Weber, M.: Evaluation of the use of five laboratory-determined ozone absorption cross sections in Brewer and Dobson retrieval algorithms, *Atmos. Chem. Phys.*, 14, 1635–1648, 2014.
- Serdyuchenko, A., Gorshchev, V., Weber, M., Chehade, W., and Burrows, J. P.: High spectral resolution ozone absorption cross-sections – Part 2: Temperature dependence, *Atmos. Meas. Tech.*, 7, 625–636, 2014.
- 5 Savastiouk, V., and McElroy, C.: Brewer spectrophotometer total ozone measurements made during the 1998 Middle Atmosphere Nitrogen Trend Assessment (MANTRA) campaign, *Atmos.–Ocean*, 43, 315–324, 2005.
- Savastiouk, V.: Improvements to the direct-sun ozone observations taken with the Brewer spectrophotometer. Ph.D. thesis, York University, Toronto, Canada, 2006.
- Schwartz, S. E., and Warneck, P.: Units for use in atmospheric chemistry, *Pure and Applied Chemistry*, 67, 1377–1406,  
10 1995.
- Sci-Tec: Brewer MKIV Spectrophotometer Operator's Manual, Saskatoon, Canada, 1999.
- Seinfeld, J. H., Pandis, S. N.: *Atmospheric chemistry and physics: From air pollution to climate change*, second edition, John Wiley & sons, inc., New Jersey, USA, 2006.
- Sellitto, P., d. Sarra, A., and Siani, A. M.: An improved algorithm for the determination of aerosol optical depth in the  
15 ultraviolet spectral range from Brewer spectrophotometer observations, *J. Opt.*, 10A, 849–855, 2006.
- Silva, A. A., and Kirchhoff, V. W. J. H.: Aerosol optical thickness from Brewer spectrophotometers and an investigation into the stray-light effect, *Appl. Opt.*, 43, 2484–2489, 2004.
- Stein-Zweers, D., and Veefkind, P.: OMI/Aura Multi-wavelength Aerosol Optical Depth and Single Scattering Albedo L3  
1 day Best Pixel in 0.25 degree x 0.25 degree V3, NASA Goddard Space Flight Center, Goddard Earth Sciences  
20 Data and Information Services Center (GES DISC), Accessed [18/04/2017] DOI:10.5067/Aura/OMI/DATA3004,  
2012.
- Unger, N., Menon, S., Koch, D. M., and Shindell, D. T.: Impacts of aerosol-cloud interactions on past and future changes in  
tropospheric composition, *Atmos. Chem. Phys.*, 9, 4115–4129, doi:10.5194/acp-9-4115-2009, 2009.
- Veefkind, P.: OMI/Aura Ozone (O3) DOAS Total Column L3 1 day 0.25 degree x 0.25 degree V3,  
25 Greenbelt, MD, USA, Goddard Earth Sciences Data and Information Services Center (GES DISC),  
Accessed [15/04/2017] DOI:10.5067/Aura/OMI/DATA3005, 2012.
- WHO: Air quality guidelines: global update 2005: particulate matter, ozone, nitrogen dioxide, and sulfur dioxide, Tech. rep.,  
World Health Organization, Geneva, Switzerland, 2006.
- WMO: Guide to meteorological instruments and methods of observation, World Meteorological Organization, WMO - No 8,  
30 7th Edn., Geneva, Switzerland, 2008.
- WMO: Scientific Assessment of Ozone Depletion: 2014, World Meteorological Organization, Global Ozone Research and  
Monitoring Project-Report No. 55, Geneva, Switzerland, 2014.